Heterogeneous reaction of peroxyacetic acid and hydrogen peroxide on ambient aerosol particles under dry and humid conditions: kinetics, mechanism and implications

Q. Q. Wu[1], L. B. Huang[1], H. Liang[1], Y. Zhao[1,a], D. Huang[1,b], and Z. M. Chen[1]

[1]State Key Laboratory of Environmental Simulation and Pollution Control, College of Environmental Sciences and Engineering, Peking University, Beijing 100871, China
[a]now at: Department of Chemistry, University of California, Irvine, CA 92697, USA
[b]now at: Department of Earth Sciences, Zhejiang University, Hangzhou, Zhejiang Province 310027, China

*Correspondence to:* Z. M. Chen (zmchen@pku.edu.cn)

Abstract. Hydrogen peroxide (H_2O_2) and organic peroxides play important roles in the cycle of oxidants and the formation of secondary aerosols in the atmosphere. Recent field observations have suggested that the budget of peroxyacetic acid (PAA, $CH_3C(O)OOH$) is potentially related to the aerosol phase processes, especially to secondary aerosol formation. Here, we present the first laboratory measurements of the uptake coefficient of gaseous PAA and H_2O_2 onto ambient fine particulate matter ($PM_{2.5}$) as a function of relative humidity (RH) at 298 K. The results show that the $PM_{2.5}$, which was collected in an urban area, can take up PAA and H_2O_2 at the uptake coefficient (γ) of 10^{-4}, and both γ_{PAA} and $\gamma_{H_2O_2}$ increase with increasing RH. The value of γ_{PAA} at 90 % RH is 5.4 ± 1.9 times that at 3 % RH, whereas $\gamma_{H_2O_2}$ at 90 % RH is 2.4 ± 0.5 times that at 3 % RH, which suggests that PAA is more sensitive to the RH variation than H_2O_2 is. Considering the larger Henry's law constant of H_2O_2 than that of PAA, the smaller RH sensitivity of the H_2O_2 uptake coefficient suggests that the enhanced uptake of peroxide compounds on $PM_{2.5}$ under humid conditions is dominated by chemical processes rather than dissolution. Considering that mineral dust is one of the main components of $PM_{2.5}$ in Beijing, we also determined the uptake coefficients of gaseous PAA and H_2O_2 on authentic Asian Dust storm (ADS) and Arizona Test Dust (ATD) particles. Compared to ambient $PM_{2.5}$, ADS shows a similar γ value and RH dependence in its uptake coefficient for PAA and H_2O_2, while ATD gives a negative dependence on RH. The present study indicates that, in addition to the mineral dust in $PM_{2.5}$, other components (e.g., soluble inorganic salts) are also important to the uptake of peroxide compounds. When the heterogeneous reaction of PAA on $PM_{2.5}$ is considered, its atmospheric lifetime is estimated to be 3.0 h on haze days and 7.1 h on non-haze days, values that are in good agreement with the field observations.

1 Introduction

Peroxide compounds, including hydrogen peroxide (H_2O_2) and organic peroxides, play an important role in the chemistry of the atmosphere, because they serve as oxidants for the conversion of S(IV) to S(VI) in the atmospheric aqueous phase, resulting in the formation of sulfate aerosol (Calvert et al., 1985; Lind et al., 1987; Stein and Saylor, 2012). Peroxide species also serve as a reservoir for HO_x (OH and HO_2) radicals (Wallington and Japar, 1990; Vaghjiani and Ravishankara, 1990; Atkinson et al., 1992; Ravetta et al., 2001) and RO_x (RO and RO_2) radicals (Lightfoot et al., 1991; Reeves and Penkett, 2003). Moreover, recent laboratory studies have indicated that peroxide compounds, especially organic peroxides, significantly contribute to the formation and aging of secondary organic aerosols (SOA) (Claeys et al., 2004; Docherty et al., 2005; Surratt et al., 2006; Paulot et al., 2009; Huang et al., 2013; Xu et al., 2014; Zhao et al., 2015).

The peroxide compounds are mainly produced by the bimolecular reaction of HO_2 and RO_2 radicals (e.g., reactions R1 and R2), and their minor sources include the ozonolysis of alkenes and biomass burning (Lee et al., 2000).

$$HO_2 + HO_2(+H_2O) \rightarrow H_2O_2 + O_2 \tag{R1}$$

$$HO_2 + CH_3C(O)OO \rightarrow CH_3C(O)OOH + O_2 \tag{R2}$$
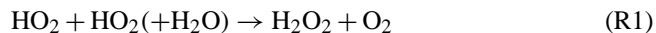
Their traditional removal pathways include reacting with OH radicals, photolysis and deposition (Lee et al., 2000). Recent studies have combined field and model data to ascertain the importance of heterogeneous loss. For example, de Reus et al. (2005) have demonstrated that, on the subtropical island, the concentration of gaseous H_2O_2 was largely overestimated by a standard gas phase chemical mechanism. When the heterogeneous uptake of H_2O_2 and/or HO_2 radicals on the surface of aerosols was accounted for in the model, the observed and modeled values were in better agreement. In addition, a series of laboratory studies have addressed the importance of the heterogeneous reaction of H_2O_2 on model or authentic mineral dust particles (Pradhan et al., 2010a, b; Wang et al., 2011; Zhao et al., 2011a, b, 2013; Romanias et al., 2012, 2013; Zhou et al., 2012; El Zein et al., 2014). For example, Pradhan et al. (2010a) have indicated that the heterogeneous reaction of H_2O_2 on dust aerosols could compete with its photolysis and significantly affect the HO_x radical budget. Romanias et al. (2012, 2013) have confirmed that the heterogeneous reaction of H_2O_2 on mineral dust had an important effect on the fate of HO_x radicals. El Zein et al. (2014) also suggested that the lifetime of H_2O_2 removed by heterogeneous reaction was comparable with its photolysis on severe dust storm periods. Our recent study has indicated that H_2O_2 could enhance the uptake of oxygenated volatile organic compounds (OVOCs) onto the surface of mineral dust particles (Zhao et al., 2014).

To the best of our knowledge, to date, there has been no laboratory experimental evidence for the importance of the heterogeneous reactions of organic peroxides in the atmosphere. As an important organic peroxide, peroxyacetic acid (PAA, $CH_3C(O)OOH$) has been frequently detected over both rural and urban areas (Lee et al., 1995; Hua et al., 2008; He et al., 2010; Zhang et al., 2010; Liang et al., 2013; Phillips et al., 2013). The typical concentration of PAA is comparable to that of H_2O_2, i.e., several tens to hundreds of pptv in summer, and the maximum concentration surpasses 1 ppbv over Mazhuang, a rural site in Shandong Province, China (Zhang et al., 2010), and the boreal forest (Phillips et al., 2013). Our field observation results have suggested that heterogeneous reactions on aerosol particles might be an important removal pathway for PAA in the atmosphere (Zhang et al., 2010; Liang et al., 2013). Therefore, we use PAA as a representative organic peroxide to investigate the kinetics and mechanisms of its heterogeneous reactions on ambient $PM_{2.5}$ as well as mineral dust particles over a wide range of relative humidities (3–90 %). We also estimate the contribution of heterogeneous reactions to the PAA budget in the atmosphere. As a comparison, we investigate the kinetics of H_2O_2 uptake on $PM_{2.5}$.

2 Experimental

2.1 Reagents and materials

Hydrogen peroxide (H_2O_2, Alfa Aesar, 35 % water solution), acetic acid (CH_3COOH, Xilong Chemical Co., LTD, 99.8 %), and sulfuric acid (H_2SO_4, Beijing Chemical Plant, 95–98 %) were used to prepare the PAA solutions. *Ortho*-phosphoric acid (H_3PO_4, Fluka, 85 %), hemin (Sigma, $\geq$ 98 %), *p*-hydroxyphenylacetic acid (POPHA, Alfa Aesar, 99 %), ammonia solution ($NH_3 \cdot H_2O$, Beijing Tongguang Fine Chemicals Company, 25.0–28.0 %), ammonium chloride (NH_4Cl, Beijing Chemical Works, $\geq$ 99.5 %), N_2 gas ($\geq$ 99.999 %, Beijing Haikeyuanchang Practical Gas Company Limited, Beijing, China), O_2 gas ($\geq$ 99.999 %, Beijing Haikeyuanchang Practical Gas Company Limited, Beijing, China) and a polytetrafluoroethylene (PTFE) filter membrane (Whatman Inc., 47 mm in diameter) were also used in the experiments. Asian Dust Storm particles (ADS particles; the BET surface area is $6.1 \, m^2 \, g^{-1}$) and Arizona Test Dust particles (ATD particles, Al Ultrafine test dust, Powder Technology; the BET surface area is $16.5 \, m^2 \, g^{-1}$) were used. ADS particles were collected at the PKU campus on 17 April 2006 after a strong sand storm. The ADS particles deposited on a glass plate and then were collected and kept in a glass bottle.

2.2 Apparatus and procedures

2.2.1 Generation of gaseous PAA and H_2O_2

PAA aqueous solution was synthesized by mixing H_2O_2 aqueous solution with acetic acid aqueous solution, using H_2SO_4 as a catalyst (Dul'neva and Moskvin, 2005; Zhao et al., 2007). The mixing aqueous solution was kept in the dark for 24 h at room temperature to make sure PAA reached its maximum balanced concentration. The PAA concentration in this primary solution (S1) was 1.3 M. The solution was stored at 277 K in the dark before use. At the beginning of every experiment, a PAA solution (S2) (4×10^{-5} M) was prepared by diluting S1 with ultrapure water and then 100 mL S2 was added into a 1 L bubbler. The S2 in the bubbler, kept in a 277 K water bath in the dark, was bubbled by a N_2 flow at a rate of 70 standard mL min^{-1} to generate gaseous PAA. The PAA-containing N_2 flow was then mixed with an O_2 flow and water vapor flow generated by another bubbler. The resulting gas mixture (reactant gas) was introduced into the filter-based flow reactor as described in Sect. 2.2.3. A H_3PO_4 solution (5×10^{-3} M) was used to scrub gaseous peroxide in a glass scrubbing coil. The collection efficiency was 85 % for PAA and 100 % for H_2O_2 at 277 K (Hua et al., 2008; Liang

et al., 2013). The peroxide-containing scrubbing solution was analyzed immediately by an online high performance liquid chromatography (HPLC, Agilent 1200). The method is described in detailed in Sect. 2.3. The concentration of PAA was 300 ± 30 pptv in the gas mixture. To ensure a constant concentration of gaseous PAA, the bubbling solution of PAA was renewed every day. The generation of gaseous H_2O_2 was similar to that of PAA. The concentration of the bubbling solution of H_2O_2 was 1.14×10^{-3} M. The resulting H_2O_2 concentration was 510 ± 40 pptv in the gas mixture.

2.2.2 Preparation of particle-loaded filters

The $PM_{2.5}$ samples were collected on the roof of a six-story teaching building (26 m above the ground) at the campus of Peking University (PKU), Beijing, China. PKU is located in the northwestern downtown area, with two major traffic arteries passing by. An ambient particulate sampler (TH–16A, Wuhan Tianhong Instruments Co., Ltd) was used to collect the $PM_{2.5}$ particles on the PTFE filters with four parallel channels operating simultaneously, and the sampling flow of each channel was 16.7 standard L min^{-1}. The $PM_{2.5}$ samples were collected for 6 days, from 31 July to 06 August 2014. Sampling was conducted twice a day for 11.5 h each time (daytime, 09:00–20:30 LT; nighttime, 21:00–08:30 LT). During the sampling period, 31 July to 03 August were haze days and 03 to 05 August were non-haze days. Haze is caused by a large number of fine particles (e.g., dust, smoke, salt) with RH less than 90 % and makes the visibility less than 10 km (Li, 2010). Here, we differentiated non-haze days from haze days based on two criteria. One was the visibility of a mountain (by eye) that is about 10 km away from the sampling site. The other was the national ambient air quality standard grade II in China, i.e., an average $PM_{2.5}$ mass concentration of lower than 75 µg m^{-3}. The $PM_{2.5}$ particle-loaded filters were sealed and kept at 255 K before use. ADS and ATD particles were separately used to prepare the mineral dust particle-loaded filters. Mineral dust particles were resuspended using a custom-built resuspension apparatus and then collected on the PTFE filters. The resuspension apparatus consists of three parts, i.e., a glass inlet, a stainless filter holder and a vacuum pump. First, we put a known number of mineral dust particles into the glass inlet and then turned off the inlet. Secondly, we turned on the vacuum pump and a negative pressure was then formed in this resuspension system. Finally, we turned on the inlet, and the particles were resuspended with the help of airflow and collected onto the filter. To compare the experimental results for $PM_{2.5}$ sampled on non-haze and haze days, the mass of ADS or ATD on the filter was carefully controlled at 0.3 and 1.3 mg for the lower and higher particle mass, respectively.

2.2.3 Uptake experiments

A filter-based flow reactor was used to measure the uptake coefficients of gaseous peroxides on aerosol particles. The schematic of this experimental apparatus is shown in Fig. 1. The reactor is composed of two perfluoroalkoxy resin filter holders (Savillex Corporation) connected in parallel. One reactor contains a blank PTFE filter, and the other contains a particle-loaded filter. The tubing system is made of Teflon tubes. The peroxide-containing gas mixture (20 % O$_2$ + 80 % N$_2$) was used at a flow rate of 2.7 standard L min^{-1} and was introduced into the blank reactor or the particle-loaded reactor via two unreactive stainless steel valves. After exiting the reactor, the peroxide-containing gas was directed into a glass scrubbing coil in a 277 ± 0.1 K water bath, in which a H_3PO_4 solution (5×10^{-3} M) was used as the eluent to scrub the peroxide at a rate of 0.2 mL min^{-1}. The same particle-loaded filter was used to measure the uptake coefficient at a continuously increasing RH ranging from 3 to 90 % and then the measurement was repeated in reverse, at a decreasing RH from 90 to 3 %. We have compared the uptake coefficients of PAA on the exposed $PM_{2.5}$ filter that has been used in the PAA uptake experiments and the unexposed $PM_{2.5}$ filter that has not been used for any experiments at 60 % RH, and no obvious difference was observed between the two uptake coefficients (Table 1). Therefore, we think the reuse of the filter for experiments at different RH has no significant effect on the results.

The uptake experiment at a certain RH took 2 h for PAA and 1 h for H_2O_2, including the time for the balance of peroxide on a blank filter and a particle-loaded filter. The balance concentrations of PAA/H_2O_2 have been detected for at least three times. Then the RH was directly changed to another RH without any treatment for the filter samples. All the experiments were conducted at 298 ± 2 K, ambient pressure and in the dark.

The uptake coefficients of gaseous peroxide can be calculated using the following equations (Molina et al., 1996; Zhao et al., 2010):

$$\gamma = \frac{\mathrm{d}\{C\}/\mathrm{d}t}{Z}, \tag{1}$$

$$Z = \frac{1}{4}\omega A_{es}[C], \tag{2}$$

$$\omega = \sqrt{\frac{8RT}{\pi M_x}}, \tag{3}$$

where $\{C\}$ is the total uptake of gaseous peroxide by particle surfaces, molecules; Z is the collision frequency, molecules s^{-1}; $[C]$ is the number concentration of gaseous peroxide, molecules m^{-3}; ω is the mean molecular speed, m s^{-1}; R is the universal gas constant, kg m^2 s^{-2} mol^{-1} K^{-1}; T is the temperature, K; A_{es} is the effective surface area of particles, m^2; M_x is the molecular weight, kg mol^{-1}. The uptake onto the particles is equal to the loss of the gaseous re-
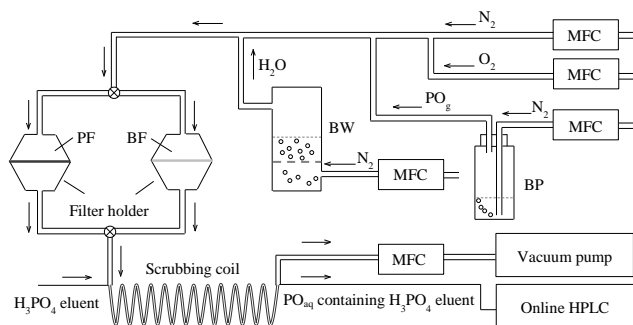
Figure 1. Schematic diagram of the experimental apparatus. MFC, mass flow controller; PF, particle-loaded filter; BF, blank filter; PO_g, gaseous peroxide compound; PO_{aq}, aqueous peroxide compound; BP, bubbler for peroxide vapor; BW, bubbler for water vapor; HPLC, high-performance liquid chromatography. The scrubbing coil, BP and BW were kept in 277 and 298 K water baths, respectively.

actant and this gas phase loss can be calculated by the difference between the reactant concentrations at the inlet and outlet of the reactor. Here, we define the fractional loss of the reactant (L_f) as Eq. (4):

$$L_f = \frac{[C]_{in} - [C]_{out}}{[C]_{in}} \qquad (4)$$

where $[C]_{in}$ and $[C]_{out}$ are the concentrations of the reactant at the inlet and outlet of the reactor, molecules m^{-3}, respectively. Since no obvious uptake of peroxide on the blank filter occurred, the reactant concentration at the outlet of the blank reactor can be treated as the initial concentration at the inlet of the reactor for the uptake on aerosols. Therefore, Eq. (1) can be expressed as Eq. (5):

$$\gamma = \frac{4 \times L_f \times V_g}{\omega A_{es}}, \qquad (5)$$

where V_g is the flow rate of the reactant-containing gas, m^3 s^{-1}. The values of γ on PM$_{2.5}$, ADS and ATD particles in the next test are calculated by the A_{es} estimated in Sect. 2.4.

2.3 Analysis of peroxides, soluble species and elements

Peroxide compounds were measured by HPLC coupled with a post-column derivatization module. The length of the column is 150 mm (Alltima AQ 5μ). The details of this method have been reported in our previous study (Hua et al., 2008). Briefly, this method is based on the determination of the fluorescent dimer produced by the reaction of POPHA and peroxides with the catalysis of hemin. The HPLC mobile phase was a H$_3$PO$_4$ solution (pH = 3.5) at a flow rate of 0.5 mL min^{-1}. The formed fluorescent dimer was analyzed by a fluorescence detector. The time of collecting a chromatogram was 10 min for PAA and 5.0 min for H$_2$O$_2$. The retention times of PAA and H$_2$O$_2$ were 8.9 and 4.0 min, respectively.

Table 1. Comparison of γ_{PAA} on exposed and unexposed PM$_{2.5}$ filters (60 % RH).

Sample	Exposed PM$_{2.5}$ particles	Unexposed PM$_{2.5}$ particles
01 Aug[a]	2.08×10^{-4}	2.03×10^{-4}
01 Aug[b]	2.29×10^{-4}	2.23×10^{-4}
05 Aug[a]	2.30×10^{-4}	2.40×10^{-4}
05 Aug[b]	2.45×10^{-4}	2.33×10^{-4}

Note: [a] daytime; [b] nighttime; exposed PM$_{2.5}$ particles, which have been used in the PAA uptake experiments; unexposed PM$_{2.5}$ filter, which has not been used for any experiments.

We used the ultrasonic method to extract the soluble compounds in particle samples. Each sample was exposed to ultrasonic treatment in ice water with 10 mL Milli-Q water for 30 min. The extracted soluble compounds were measured by ion chromatography (IC, Dionex ICS2000 and ICS2500). The analytical columns for cations and anions were Dionex CS 12A and Dionex AS 11, respectively. Here, the measured compounds include eight inorganic ions (i.e., K$^+$, Ca^{2+}, Na$^+$, Mg^{2+}, NH$_4^+$, Cl$^-$, NO$_3^-$ and SO$_4^{2-}$) and four organic acids (i.e., formic acid, acetic acid, pyruvic acid and oxalic acid).

We used acid digestion to extract elements in particles through a microwave digestion system (CEM MARS, USA). Elements in the extractions were measured by inductively coupled plasma mass spectroscopy (ICP-MS, Thermo X series). The measured elements include Mg, Al, P, Ca, Ti, V, Cr, Mn, Fe, Co, Ni, Cu, Zn, As, Se, Mo, Cd, Ba, Tl, Pb, Th and U.

2.4 Estimation of effective surface area

The effective surface area (A_{es}) is a key factor in the uptake of a specific compound from the gas phase onto aerosol particles. The uptake coefficient (γ) estimated by the geometric filter surface area (A_{gs}) is several orders of magnitude higher than that by the Brunauer–Emmett–Teller (BET) surface area (Shen et al., 2013). To date, accurate estimation of A_{es} of the particle sample has been a challenge for the determination of γ. Bedjanian et al. (2013) have measured the uptake of HO$_2$ radicals on ATD particles and showed a pseudo-logarithmic relationship between the uptake and the particle mass. In the present study, ambient particles were loaded on the filter in an agglomerated state, extremely different from their status in the atmosphere, where they are highly dispersed. Obviously, neither the geometric surface area nor the BET surface area can represent the A_{es} of the ambient particle samples on the filter. Here, we estimated A_{es} by investigating the relationship between the uptake and loaded particle mass. Eq. (5) shows that the fractional loss (L_f) of a specific gaseous reactant due to the uptake of the filter-loaded particles was directly proportional to A_{es}. The value of A_{es} should depend on the loaded particle mass. Therefore, we used the relationship between L_f and particle mass (M_a) to estimate the value of A_{es}. Figure 2 shows the relationship between the L_f of
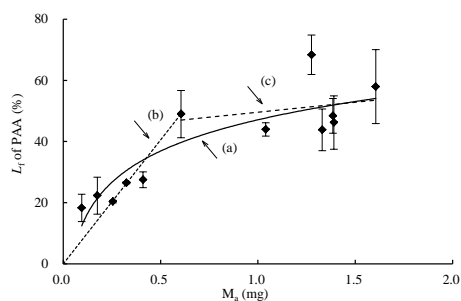
Figure 2. The trend line of fractional loss (L_f) of PAA against PM$_{2.5}$ mass (M_a) (60 % RH). Error bars are 1 standard deviation. Solid line (a), the logarithmic trend line of L_f against M_a among all mass values; dotted line (b), the linear correlation of L_f against M_a in the low mass region; dotted line (c), the nearly constant L_f against M_a in the high mass region.

gaseous PAA versus the loaded particle mass. Although L_f appeared to have a linear relationship with particle mass in the low particle mass region, it generally fit with the logarithmic function of particle mass, with a correlation coefficient $r = 0.88$. This empirical logarithmic relationship is given in Eqs. (6) to (8):

$$\text{For PM}_{2.5}\, L_f = 0.15 \times \ln(M_a) + 0.47, \tag{6}$$

$$\text{For ADS}\, L_f = 0.099 \times \ln(M_a) + 0.26, \tag{7}$$

$$\text{For ATD}\, L_f = 0.058 \times \ln(M_a) + 0.20, \tag{8}$$

where M_a is the mass of the particles, mg. The mass used for measuring the L_f of ADS is 0.18, 0.37, 0.81, 1.05, 1.16, 1.63, 1.86 and 2.46 mg, respectively. The mass for measuring the L_f of ATD is 0.27, 0.48, 0.83, 1.07, 1.36, 1.58, 1.76, 2.02, 2.57 and 3.00 mg, respectively. In the low particle mass region, the particles were highly dispersed on the filter and A_{es} increased rapidly with increasing particle mass; in the high particle mass region, particles highly overlapped and agglomerated with each other on the filter, and A_{es} was closer to A_{gs} (12.43 cm^2). Here, we assume that there exists a critical particle mass ($M_{a,c}$) for which A_{es} is equal to A_{gs}. When the particle mass is greater than $M_{a,c}$, A_{es} tends to be constant, i.e., the A_{gs}. For $M_{a,c}$, the corresponding fractional loss of PAA is L_{f_c}. We used an iterative method to determine $M_{a,c}$. The termination criterion of this iterative method was the relative error (R_{el}) of L_{f_c} towards the average of all the L_f values ($\overline{L_f}$) that were larger than L_{f_c} and the calculation method was expressed in Eq. (9). Here, we set R_{el} as 5 % to terminate the iteration. The procedure of the iteration was as follows: (i) start $M_{a,c}$ with 0.10 mg; (ii) calculate series values of L_f by inputting a range of M_a (0.01 to 2.00 mg) into Eq. (6); (iii) calculate R_{el} by the calculated values of L_f and Eq. (9); (iv) if R_{el} is larger than 5 %, reset $M_{a,c}$ with an added mass of 0.01 mg (i.e., 0.11 mg); (v) repeat steps (ii–iv) until R_{el} is less than 5 %, and then obtain the expected $M_{a,c}$ and L_{f_c}. The

Table 2. Summary of the collected mass and effective surface area of PM$_{2.5}$ on the filter, and its ambient average mass concentrations on haze and non-haze days.

Samples	Weather	M_a (mg)	Concentration (μg m^{-3})	A_{es} (cm^2)
31 Jul[a]	Haze	1.28	127.0	12.88
31 Jul[b]	Haze	1.61	156.9	13.75
01 Aug[a]	Haze	1.33	132.6	13.04
01 Aug[b]	Haze	1.39	136.7	13.19
02 Aug[a]	Haze	1.04	107.0	12.12
02 Aug[b]	Haze	1.39	137.8	13.21
03 Aug[a]	Haze → non-haze	0.60	61.7	10.09
03 Aug[b]	Non-haze	0.41	41.1	8.63
04 Aug[a]	Non-haze	0.10	9.2	3.15
04 Aug[b]	Non-haze	0.18	16.9	5.44
05 Aug[a]	Non-haze	0.26	25.6	6.85
05 Aug[b]	Non-haze	0.32	32.4	7.76

Note: [a] daytime; [b] nighttime; A_{es}, effective surface area; M_a, mass of PM$_{2.5}$.

calculated L_{f_c} was 4.89×10^{-1}, which was similar to the experimental result in Fig. 2., i.e., 4.90×10^{-1}. Based on the directly proportional relationship between A_{es} and L_f, A_{es} can be expressed in Eq. (10).

$$R_{el} = \frac{L_{f_c}}{\overline{L_f}} \tag{9}$$

$$A_{es} = \frac{A_{gs}}{L_{f_c}} \times L_f \tag{10}$$

The estimation of A_{es} for filter-loaded PM$_{2.5}$, ADS and ATD particles can be expressed as the respective logarithmic functions in Eqs. (11) to (13):

$$\text{For PM}_{2.5}\, A_{es} = 3.75 \times \ln(M_a) + 12.0, \tag{11}$$

$$\text{For ADS}\, A_{es} = 3.66 \times \ln(M_a) + 9.59, \tag{12}$$

$$\text{For ATD}\, A_{es} = 3.01 \times \ln(M_a) + 10.3, \tag{13}$$

where M_a represents the filter-loaded particle mass, mg; A_{es} represents the effective surface area of particles, cm^2. The mass of the filter-loaded PM$_{2.5}$ and the estimated A_{es} values are listed in Table 2. A_{es} for PM$_{2.5}$ changes with the particle mass, ranging from 3.2 to 13.8 cm^2; A_{es} for ADS is 6.1 and 10.9 cm^2, respectively; A_{es} for ATD is 6.4 and 11.2 cm^2, respectively. The uptake coefficients on PM$_{2.5}$ particles, ADS and ATD particles below are all calculated with these A_{es} values.

3 Results and discussion

3.1 Uptake of PAA and H$_2$O$_2$ on PM$_{2.5}$

The uptake coefficient of PAA (γ_{PAA}) on PM$_{2.5}$ particles was measured over a wide range of RH (3–90 %). Figure 3 shows the γ_{PAA} profile on PM$_{2.5}$ with respect to increasing/decreasing RH. γ_{PAA} increases with increasing RH on

Table 3. The uptake coefficients γ ($\times 10^{-4}$) of PAA on $PM_{2.5}$, ADS, and ATD under different relative humidity conditions. The values in the parentheses are the lower limit of γ ($\times 10^{-5}$).

RH	$PM_{2.5h}$	$PM_{2.5n}$	ADS_l	ADS_h	ATD_l	ATD_h
3 %	0.81 ± 0.26	0.98 ± 0.27	0.84 ± 0.01	1.37 ± 0.02	2.42 ± 0.02	1.86 ± 0.01
	$(0.23 \pm 0.06)^a$	$(0.54 \pm 0.24)^a$	$(2.19 \pm 0.27)^b$	$(1.72 \pm 0.02)^b$	$(3.45 \pm 0.03)^b$	$(0.93 \pm 0.02l)^b$
20 %	1.37 ± 0.20	1.41 ± 0.38	1.26 ± 0.03	1.78 ± 0.03	2.15 ± 0.05	1.44 ± 0.03
	$(0.40 \pm 0.11)^a$	$(0.78 \pm 0.33)^a$	$(3.27 \pm 0.38)^b$	$(2.24 \pm 0.04)^b$	$(3.07 \pm 0.07)^b$	$(0.72 \pm 0.05)^b$
40 %	1.95 ± 0.52	1.99 ± 0.52	1.65 ± 0.08	2.11 ± 0.06	1.81 ± 0.03	1.27 ± 0.03
	$(0.58 \pm 0.24)^a$	$(1.11 \pm 0.46)^a$	$(4.28 \pm 0.5)^b$	$(2.66 \pm 0.08)^b$	$(2.59 \pm 0.04)^b$	$(0.64 \pm 0.03)^b$
60 %	2.76 ± 0.54	2.63 ± 0.70	2.26 ± 0.08	2.39 ± 0.04	1.62 ± 0.01	1.16 ± 0.02
	$(0.83 \pm 0.32)^a$	$(1.47 \pm 0.63)^a$	$(5.86 \pm 0.70)^b$	$(3.01 \pm 0.06)^b$	$(2.31 \pm 0.02)^b$	$(0.58 \pm 0.01)^b$
75 %	3.43 ± 0.63	3.42 ± 1.25	2.60 ± 0.03	2.55 ± 0.01	1.47 ± 0.01	1.07 ± 0.03
	$(1.03 \pm 0.38)^a$	$(1.92 \pm 1.00)^a$	$(6.74 \pm 1.25)^b$	$(3.21 \pm 0.01)^b$	$(2.1 \pm 0.002)^b$	$(0.53 \pm 0002)^b$
90 %	4.20 ± 0.58	4.63 ± 1.30	3.21 ± 0.08	2.62 ± 0.01	1.17 ± 0.03	0.91 ± 0.04
	$(1.24 \pm 0.41)^a$	$(2.60 \pm 1.09)^a$	$(8.32 \pm 1.30)^b$	$(3.30 \pm 0.01)^b$	$(1.67 \pm 0.04)^b$	$(0.45 \pm 0.03)^b$

Note: $PM_{2.5h}$, haze day $PM_{2.5}$; $PM_{2.5n}$, non-haze day $PM_{2.5}$; ADS_h and ATD_h, the mass of mineral dust about 1.3 mg; ADS_l and ATD_l, the mass of mineral dust, about 0.3 mg; [a] uptake coefficient calculated by total surface area of the particles using size distribution, representing the lower limit; [b] uptake coefficient calculated by BET area, representing the lower limit; the errors represent the relative standard deviation between γ on particles of ascending and descending RH.

both daytime and nighttime $PM_{2.5}$ samples. The values of γ_{PAA} on nighttime $PM_{2.5}$ samples are similar to those on daytime $PM_{2.5}$ samples. Additionally, although the mass of $PM_{2.5}$ collected on a haze day is significantly different from that on a non-haze day, the γ_{PAA} values are similar under these two different weather conditions (Table 3). In general, γ_{PAA} rises from $(0.89 \pm 0.26) \times 10^{-4}$ at 3 % RH to $(4.41 \pm 0.92) \times 10^{-4}$ at 90 % RH. Table 3 also lists the lower limit of γ_{PAA} on $PM_{2.5}$, which are calculated using the total surface area of the particles using size distribution (see the details in Sect. 4, and Eqs. 21 and 22). The lower limit is on the order of 10^{-6}–10^{-5}. The empirical equation of γ_{PAA} plotted against water activity (a_{H_2O}; here, $a_{H_2O} = \text{RH}/100$) can be expressed as Eq. (14) and the measured and modeled γ_{PAA} on $PM_{2.5}$ are shown in Fig. 4.

$$\gamma_{PAA} = \frac{4.94 \times 10^{-5}}{1 - 0.91 \times a_{H_2O}^{0.21}} \tag{14}$$

We also determined the uptake coefficients of H_2O_2 on $PM_{2.5}$ over the RH range of 3 to 90 %. Before this experiment, we compared the measured uptake coefficients of H_2O_2 on two $PM_{2.5}$ samples; one had been used to measure the uptake coefficient of PAA and the other had not been used for any measurements. The results show that the relative error between the above two experiments was 1.0–7.4 % among different RH (3–90 %). Therefore, there is no obvious difference between the uptake coefficients of H_2O_2 on used and unused $PM_{2.5}$ samples. Figure 5 shows the $\gamma_{H_2O_2}$ on $PM_{2.5}$ that had been used to measure γ_{PAA}, over 3–90 % RH. The empirical equation of $\gamma_{H_2O_2}$ as a function of a_{H_2O} can be expressed as Eq. (15) and the measured and modeled $\gamma_{H_2O_2}$ on

$PM_{2.5}$ is shown in Fig. 4.

$$\gamma_{H_2O_2} = \frac{5.32 \times 10^{-4}}{1 - 0.82 \times a_{H_2O}^{0.13}} \tag{15}$$

The value of $\gamma_{H_2O_2}$, similar to γ_{PAA}, shows a positive correlation with RH. The average value of $\gamma_{H_2O_2}$ changes from $(1.12 \pm 0.20) \times 10^{-4}$ at 3 % RH to $(2.70 \pm 0.37) \times 10^{-4}$ at 90 % RH. The positive RH dependence of $\gamma_{H_2O_2}$ has been reported by Pradhan et al. (2010b). They have measured $\gamma_{H_2O_2}$ on authentic mineral dust particles (i.e., Gobi dust particles and Saharan dust particles). Table 4 summarizes the literature result of $\gamma_{H_2O_2}$ and its RH dependence on different types of mineral dust. Apart from $\gamma_{H_2O_2}$ on authentic Gobi dust, authentic Saharan dust and aged particles, all $\gamma_{H_2O_2}$ values show a negative RH dependence.

Figure 6 shows the ratios of $\gamma_{PAA,90\%\,RH}$ to $\gamma_{PAA,3\%\,RH}$ ($R_{\gamma PAA}$) and $\gamma_{H_2O_2,90\%\,RH}$ to $\gamma_{H_2O_2,3\%\,RH}$ ($R_{\gamma H_2O_2}$). Although the $R_{\gamma PAA}$ values are more variable on haze days than those on non-haze days, the average value of $R_{\gamma PAA}$ shows no obvious difference at different times and under different weather conditions, varying over the narrow range of 4.4 ± 0.6 to 6.3 ± 2.7. On average, $R_{\gamma PAA}$ is 5.4 ± 1.9. It is interesting to note that $R_{\gamma H_2O_2}$ is 2.4 ± 0.5 (see Fig. 6b), which is much lower than $R_{\gamma PAA}$. Although $\gamma_{H_2O_2}$ has a positive RH dependence on $PM_{2.5}$ as well, H_2O_2 is less sensitive to RH variance compared to PAA. For peroxide compounds, if a physical process, especially the dissolution, dominates their uptake on $PM_{2.5}$, the $R_{\gamma H_2O_2}$ should be larger than $R_{\gamma PAA}$, because the Henry's law constant of H_2O_2 is 100 times larger than that of PAA (298 K) (8.47×10^2 M atm^{-1} for PAA and 8.43×10^4 M atm^{-1} for H_2O_2) (O'Sullivan et al., 1996). This expectation, however, is at odds with our experimental results. Hence, we speculate that the physical pro-

Table 4. Summary of the uptake coefficients of H_2O_2 on mineral dust particles in literature data.

Substrate	RH dependence	Uptake coefficient	Method	Reference
TiO_2	N	$(1.53 \pm 0.11) \times 10^{-4}$–$(5.04 \pm 0.58) \times 10^{-4}$	AFT-CIMS	Pradhan et al. (2010a)
Gobi dust	P	$(3.33 \pm 0.26) \times 10^{-4}$–$(6.03 \pm 0.42) \times 10^{-4}$	AFT-CIMS	Pradhan et al. (2010b)
Saharan dust		$(6.20 \pm 0.22) \times 10^{-4}$–$(9.42 \pm 0.41) \times 10^{-4}$		
Al_2O_3	N	$(1.21 \pm 0.04) \times 10^{-8}$–$(0.76 \pm 0.09) \times 10^{-7}$	T-FTIR	Zhao et al. (2011a)
SiO_2	N	$(1.55 \pm 0.14) \times 10^{-8}$–$(0.61 \pm 0.06) \times 10^{-7}$	T-FTIR	Zhao et al. (2011b)
HNO_3–Al_2O_3	N ($< 75\%$); P ($> 75\%$)	$\gamma_{aged}/\gamma_{pristine} = 0.5$–$1.1$		
SO_2–Al_2O_3	P	$\gamma_{aged}/\gamma_{pristine} = 1.2$–$1.9$		
SiO_2	–	$\gamma_0 = (5.22 \pm 0.9) \times 10^{-5}$	Knudsen cell QMS	Wang et al. (2011)
Al_2O_3		$\gamma_0 = (1.00 \pm 0.11) \times 10^{-4}$		
Fe_2O_3		$\gamma_0 = (9.70 \pm 1.95) \times 10^{-5}$		
MgO		$\gamma_0 = (1.66 \pm 0.23) \times 10^{-4}$		
TiO_2	N	$\gamma_{0,dark} = \dfrac{4.1 \times 10^{-3}}{1 + RH^{0.65}}$	CWFT-QMS	Romanias et al. (2012)
SiO_2	–	$\gamma_0 = \dfrac{\exp(934.5/T - 12.7)}{1 + \exp(934.5/T - 12.7)}$	Knudsen cell QMS	Zhou et al. (2012)
$CaCO_3$		$\gamma_0 = \dfrac{\exp(1193.0/T - 11.9)}{1 + \exp(1193.0/T - 11.9)}$		
HNO_3–$CaCO_3$	P	$\gamma_{aged}/\gamma_{pristine} = 1 - 8$	T-FTIR	Zhao et al. (2013)
SO_2–$CaCO_3$	P	$\gamma_{aged}/\gamma_{pristine} = 3 - 10$		
Al_2O_3	N	$\gamma_0 = \dfrac{1.10 \times 10^{-3}}{1 + RH^{0.93}}$	CWFT-QMS	Romanias et al. (2013)
Fe_2O_3	N	$\gamma_0 = \dfrac{1.05 \times 10^{-3}}{1 + RH^{0.73}}$		
ATD	N	$\gamma_0 = \dfrac{4.8 \times 10^{-4}}{1 + RH^{0.66}}$	CWFT-QMS	El Zein et al. (2014)

Note: N, negative RH dependence; P, positive RH dependence; γ_0, initial uptake coefficient; AFT, aerosol flow tube; CIMS, chemical ionization mass spectrometer; T-FTIR, transmission Fourier transform infrared spectroscopy; QMS, quadrupole mass spectrometer; CWFT, coated-wall flow tube.

cess is not the main pathway for the uptake of peroxide compounds on $PM_{2.5}$. In addition, the values of γ_{PAA} and $\gamma_{H_2O_2}$ on $PM_{2.5}$ were measured with increasing RH from 3 to 90 % and then the measurements were repeated by using the same sample with decreasing RH from 90 to 3 %. Interestingly, we find that the γ_{PAA} and $\gamma_{H_2O_2}$ can be well repeated in these two cases (see Figs. 3 and 5). The independence of γ_{PAA} and $\gamma_{H_2O_2}$ from reaction time also indicates that $PM_{2.5}$ has a sustained reactivity for the uptake of peroxide compounds at different RH, which falls into the category of reactive uptake as suggested by Crowley et al. (2010). The detailed mechanism is described in Sect. 3.3.

The present study is the first investigation on the kinetics of the heterogeneous reactions of PAA and H_2O_2 on $PM_{2.5}$ particles. Recent studies have already indicated the importance of mineral dust for H_2O_2 uptake (Pradhan et al., 2010a, b; Wang et al., 2011; Zhao et al., 2011a, b, 2013; Romanias et al., 2012, 2013; Zhou et al., 2012; El Zein et al., 2014). For PAA, however, no data regarding its kinetics on mineral dust have been available in the literature. Therefore, we investigated the heterogeneous reaction of PAA on mineral dust as a comparison of that on $PM_{2.5}$.

3.2 Uptake of PAA and H_2O_2 on mineral dust

Mineral dust is an important component of atmospheric aerosols in Beijing; it comprises 6.0 and 6.2 % of $PM_{2.5}$ on haze days and non-haze days, which is similar to the reported values (7.1–12.9 %) (Sun et al., 2004; Yang et al., 2011; Zhang et al., 2013). To determine whether the mineral dust dominates the uptake of PAA on $PM_{2.5}$, we measured the γ_{PAA} on two kinds of mineral dust particles, i.e., ADS and ATD particles. The measured γ_{PAA} values are listed in Table 3. γ_{PAA} on low mass ADS (ADS$_l$) increases from $(0.84 \pm 0.01) \times 10^{-4}$ at 3 % RH to $(3.21 \pm 0.08) \times 10^{-4}$ at 90 % RH and γ_{PAA} on high mass ADS (ADS$_h$) increases from $(1.37 \pm 0.02) \times 10^{-4}$ at 3 % RH to $(2.62 \pm 0.01) \times 10^{-4}$ at 90 % RH. On the surface of ATD, however, γ_{PAA} shows a negative RH dependence, from $(2.42 \pm 0.02) \times 10^{-4}$ at 3 % RH to $(1.17 \pm 0.03) \times 10^{-4}$ at 90 % RH on low mass ATD (ATD$_l$) and decreasing from $(1.86 \pm 0.01) \times 10^{-4}$ at 3 % RH to $(0.91 \pm 0.04) \times 10^{-4}$ at 90 % RH on high mass ATD (ATD$_h$). Table 3 also lists the lower limit of γ_{PAA} on ADS and ATD, which are calculated by the BET surface area of the particles. The lower limits of γ_{PAA} on ADS and ATD are on the order of 10^{-6}–10^{-5}. The positive correlations between RH and γ_{PAA} on ADS are similar to that on $PM_{2.5}$. Similar positive RH dependence has also been observed for the uptake of H_2O_2 on authentic Gobi dust,
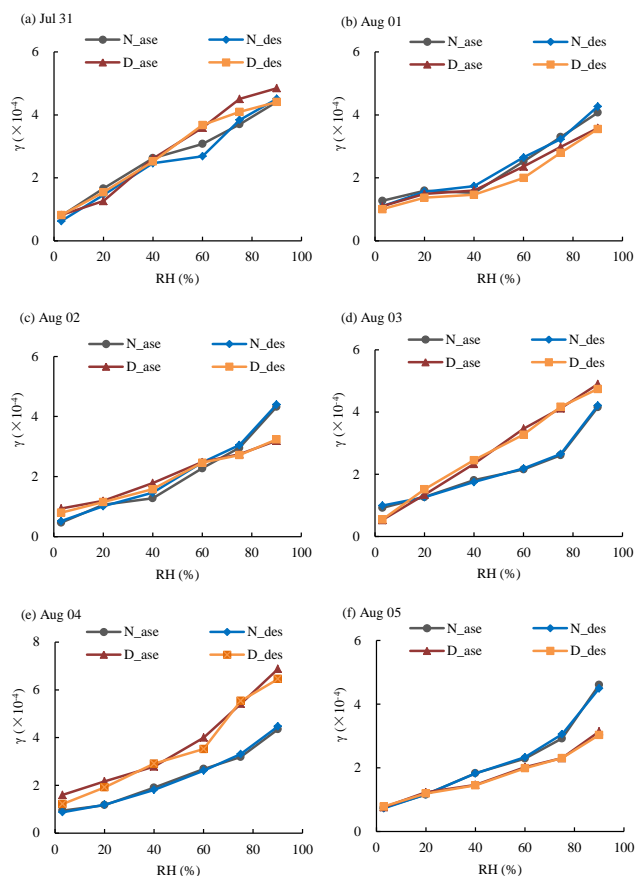
Figure 3. Profiles of uptake coefficients of gaseous PAA on $PM_{2.5}$ over a range of RH (3–90 %); N_ase, γ_{PAA} was measured with ascending RH on nighttime $PM_{2.5}$ particles; N_des, γ_{PAA} was measured with descending RH on nighttime $PM_{2.5}$ particles; D_ase, γ_{PAA} was measured with ascending RH on daytime $PM_{2.5}$ particles; D_des, γ_{PAA} was measured with descending RH on daytime $PM_{2.5}$ particles.

Saharan dust (Pradhan et al., 2010b) and aged $CaCO_3$ particles (Zhao et al., 2013). This negative RH dependence on ATD is similar to the previously reported $\gamma_{H_2O_2}$ on ATD and mineral oxides (e.g., α–Al_2O_3, Fe_2O_3, TiO_2, SiO_2) (Pradhan et al., 2010a; Zhao et al., 2011a; Romanias et al., 2012, 2013; El Zein et al., 2014). The reasons for the discrepancies in the RH dependence of γ_{PAA} are discussed in Sect. 3.3. The empirical equation of γ_{PAA} against a_{H_2O} on ADS and ATD can be expressed as Eqs. (16) and (17), respectively:

$$\gamma_{PAA} = \frac{7.49 \times 10^{-5}}{1 - 0.76 \times a_{H_2O}^{0.25}}, \tag{16}$$

$$\gamma_{PAA} = \frac{2.18 \times 10^{-4}}{1 + 1.08 \times a_{H_2O}^{1.06}}. \tag{17}$$

We also determined the uptake coefficient of H_2O_2 on ADS and ATD over the RH range of 3 to 90 %. The measured $\gamma_{H_2O_2}$ on ADS and ATD is shown in Fig. 7. The

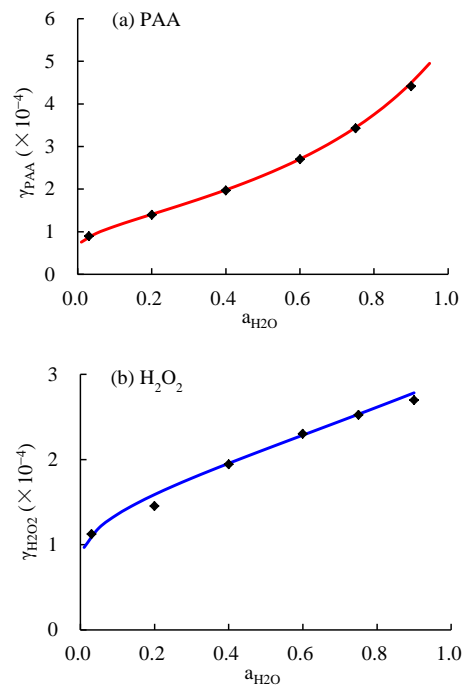**Figure 4.** The uptake coefficients of PAA and H_2O_2 on $PM_{2.5}$ particles. The red line and the blue line in **(a)** and **(b)** represent the empirical fit of γ_{PAA} and $\gamma_{H_2O_2}$, respectively.

value of $\gamma_{H_2O_2}$, similar to γ_{PAA}, shows a positive correlation with RH on ADS particles and a negative correlation with RH on ATD particles. By taking the average of γ values at low and high mass loading, $\gamma_{H_2O_2}$ on ADS increases from $(1.10 \pm 0.31) \times 10^{-4}$ at 3 % RH to $(2.44 \pm 0.69) \times 10^{-4}$ at 90 % RH and the $\gamma_{H_2O_2}$ on ATD decreases from $(3.11 \pm 0.34) \times 10^{-4}$ at 3 % RH to $(0.87 \pm 0.06) \times 10^{-4}$ at 90 % RH. Although the values of $\gamma_{H_2O_2}$ at low and high mass loading are not identical, all $\gamma_{H_2O_2}$ values on ADS show a positive correlation with RH, and all $\gamma_{H_2O_2}$ values on ATD show a negative correlation with RH. A_{es} for ADS_l and ADS_h is 6.1 and 10.9 cm^2, respectively; A_{es} for ATD_l and ATD_h is 6.4 and 11.2 cm^2, respectively.

The empirical equation of γ_{PAA} against a_{H_2O} on ADS and ATD can be expressed as Eqs. (18) and (19), respectively:

$$\gamma_{H_2O_2} = \frac{9.97 \times 10^{-5}}{1 - 0.63 \times a_{H_2O}^{0.59}}, \tag{18}$$

$$\gamma_{H_2O_2} = \frac{3.33 \times 10^{-4}}{1 + 3.02 \times a_{H_2O}^{1.07}}. \tag{19}$$

It is noted that, although the γ values of H_2O_2 and PAA on mineral dust particles obtained with the low mass loading are not the same with those with high mass loading, they have the same RH dependence. The differences among ADS_l, ADS_h, ATD_l and ATD_h are mainly caused by two reasons: the un-
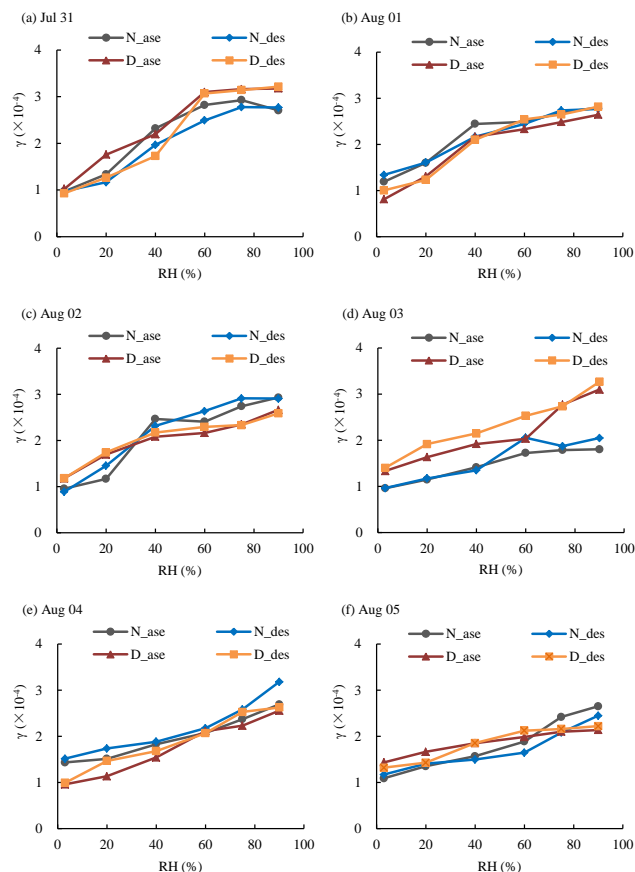
Figure 5. Profiles of uptake coefficient of gaseous H_2O_2 on $PM_{2.5}$ over a range of RH (3–90 %); N_ase, $\gamma_{H_2O_2}$ was measured with ascending RH on nighttime $PM_{2.5}$ particles; N_des, $\gamma_{H_2O_2}$ was measured with descending RH on nighttime $PM_{2.5}$ particles; D_ase, $\gamma_{H_2O_2}$ was measured with ascending RH on daytime $PM_{2.5}$ particles; D_des, $\gamma_{H_2O_2}$ was measured with descending RH on daytime $PM_{2.5}$ particles.

certainty of the A_{es} estimation method and the experimental error.

3.3 Reaction mechanisms

In general, the uptake of a gas onto particles can be attributed to physical processes (e.g., physisorption and dissolution) and/or chemical processes (e.g., catalytic reaction, acid–base reaction, redox reaction and thermal decomposition). In Sect. 3.1, we have provided evidence that the chemical processes dominate the uptake of peroxide compounds on $PM_{2.5}$. Here, we discuss the potential chemical pathways.

The composition of $PM_{2.5}$ determines the relative importance of physical and chemical processes. In general, $PM_{2.5}$ is mainly composed of mineral dust, sulfate, nitrate, ammonium compounds, soot and organic matter (Eldred et al., 1997; He et al., 2001; Hueglin et al., 2005; Sun et al., 2006; Huang et al., 2014). In this study, we have measured the con-
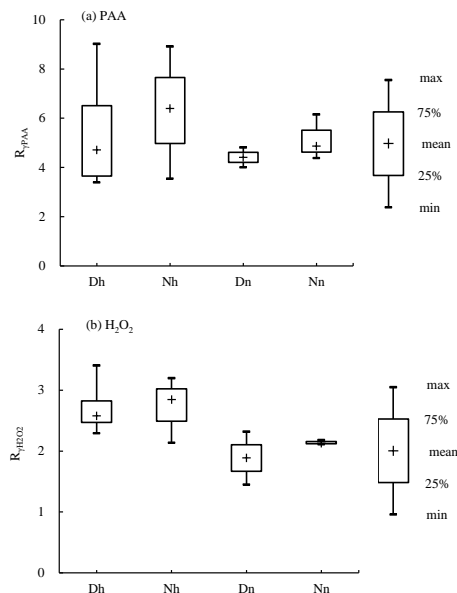

Figure 6. The ratio of γ at 90 % RH to γ at 3 % RH ($R_{\gamma PAA}$ and $R_{\gamma H_2O_2}$) on $PM_{2.5}$. Dh, daytime of haze day; Nh, nighttime of haze day; Dn, daytime of non-haze day; Nn, nighttime of non-haze day.

centrations of elements and soluble ions in $PM_{2.5}$ samples. The results are shown in Table 5. The concentration of mineral dust was estimated by multiplying 14.3 by the concentration of the Al element; the ratio was suggested by Zhang et al. (2013) for $PM_{2.5}$ in urban Beijing. The estimated mineral dust accounts for 6.0 ± 4.3 and 6.2 ± 3.1 % of $PM_{2.5}$ mass concentration on haze days and non-haze days, respectively. The concentration of SO_4^{2-} is $42.26 \pm 7.88\,\mu g\,m^{-3}$ on haze days, which is about 7 times that on non-haze days. The concentrations of NO_3^- and Cl^- on haze days are also about 6.9–7.3 times those on non-haze days.

There have been several studies of the mechanism of H_2O_2 uptake on mineral dust particles. Zhao et al. (2011a) have found that the uptake of H_2O_2 on both SiO_2 and $\alpha-Al_2O_3$ particles decreased with increasing RH. On SiO_2 particles, the contribution of physisorption to H_2O_2 uptake increased from 59 % at 12 % RH to 80 % at 76 % RH; on $\alpha-Al_2O_3$ particles, the catalytic decomposition dominated H_2O_2 uptake even at high RH, probably due to its high surface reactivity. Although the $\gamma_{H_2O_2}$ on both SiO_2 and $\alpha-Al_2O_3$ particles decreased with increasing RH, the reduction was more pronounced on the physical process dominated SiO_2 particles. El Zein et al. (2014) observed a negative correlation between RH and $\gamma_{H_2O_2}$ on ATD particles and suggested that the uptake of H_2O_2 on ATD particles was a catalytic process and that it was not limited by site-filling. Thus, the catalytic reaction of mineral dust might be important to the uptake of peroxide compounds on $PM_{2.5}$. But this reaction alone cannot explain the positive RH dependence for the γ on $PM_{2.5}$. Therefore, some other pathways may also be important to the uptake of
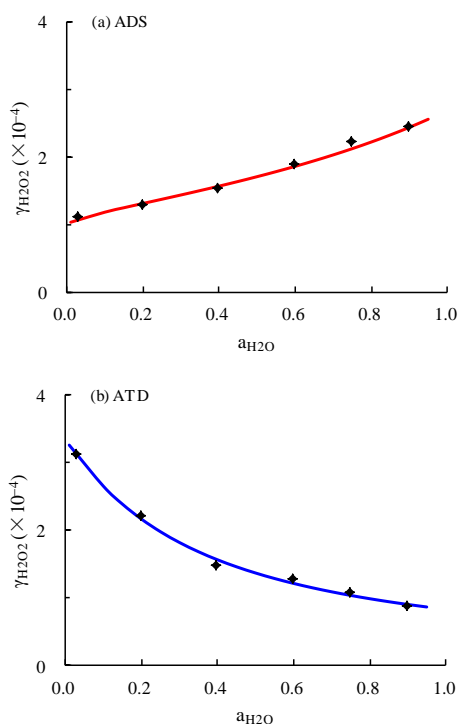
Figure 7. Uptake coefficient of H_2O_2 on ADS and ATD particles. The red line and the blue line in **(a)** and **(b)** represent the empirical fit of $\gamma_{H_2O_2}$ on ADS and ATD particles, respectively.

Table 5. The average concentration of ions, organic acids and elements of $PM_{2.5}$ on haze and non-haze days. The errors represent the relative standard deviation.

Species	Haze day	Non-haze day
SO_4^{2-},[a]	42.3 ± 7.88	5.95 ± 5.88
NO_3^-,[a]	23.2 ± 16.8	3.18 ± 2.92
Cl^-,[a]	1.07 ± 1.48	0.15 ± 0.12
NH_4^+,[a]	6.11 ± 1.22	1.51 ± 1.01
K^+,[a]	1.10 ± 0.27	0.26 ± 0.16
Na^+,[a]	0.49 ± 0.15	0.24 ± 0.11
HO(O)CC(O)OH[a]	0.83 ± 0.06	0.21 ± 0.10
HC(O)OH[a]	0.20 ± 0.09	0.07 ± 0.06
CH_3C(O)OH[a]	0.19 ± 0.16	0.16 ± 0.32
CH_3C(O)C(O)OH[a]	0.04 ± 0.01	0.01 ± 0.01
Al[a]	0.45 ± 0.36	0.10 ± 0.09
Ca[a]	0.44 ± 0.16	0.30 ± 0.14
Mg[a]	0.10 ± 0.04	0.05 ± 0.03
P[a]	0.19 ± 0.12	0.14 ± 0.19
Fe[a]	0.60 ± 0.14	0.17 ± 0.10
Ti[a]	0.04 ± 0.01	0.03 ± 0.03
Mn[a]	0.03 ± 0.01	0.01 ± 0.01
Cu[a]	0.03 ± 0.02	0.01 ± 0.01
Zn[a]	0.18 ± 0.08	0.03 ± 0.02
V[a]	0.01 ± 0.01	0.01 ± 0.01
Pb[a]	0.08 ± 0.02	0.01 ± 0.01
Ba[b]	10.22 ± 3.06	3.68 ± 1.76
Cr[b]	8.55 ± 2.58	4.16 ± 2.49
Se[b]	4.56 ± 1.60	1.28 ± 0.95
Ni[b]	4.54 ± 1.88	0.44 ± 0.30
As[b]	4.30 ± 2.64	5.57 ± 3.63
Mo[b]	1.16 ± 0.50	0.42 ± 0.20
Tl[b]	1.12 ± 0.41	0.14 ± 0.10
Cd[b]	1.09 ± 0.32	0.22 ± 0.17
Co[b]	0.40 ± 0.10	0.19 ± 0.08
U[b]	0.04 ± 0.01	0.02 ± 0.02
Th[b]	0.03 ± 0.02	0.01 ± 0.02

Note: [a] the unit is $\mu g\,m^{-3}$; [b] the unit is $ng\,m^{-3}$.

peroxide compounds onto $PM_{2.5}$. Based on the characteristics of peroxide compounds, in addition to catalytic reaction, acid–base reaction, redox reaction, thermal decomposition, and aqueous reaction are considered as the potential pathways.

With respect to acid–base reactions, we must consider that H_2O_2 and PAA are both weak acids ($pK_a = 11.6$ for H_2O_2, Marinoni et al., 2011; $pK_a = 8.2$ for PAA, Evans and Upton, 1985) and can react with alkaline substances. A number of studies have demonstrated that the heterogeneous reaction of an acidic vapor on alkaline materials is enhanced with increasing RH (Santschi and Rossi, 2006; Preszler et al., 2007; Sullivan et al., 2009). However, $PM_{2.5}$ in Beijing is acidic (e.g., pH = 5.57, Wang et al., 2005). The concentrations of ions of strong acids such as SO_4^{2-} and NO_3^- make up 60.9 % of $PM_{2.5}$ mass on haze days, and 41.3 % on non-haze days (see Table 5). Even though there are some basic components (such as NH_4^+ and $CaCO_3$), we believe they are already neutralized or acidified. Therefore, acid–base reactions on $PM_{2.5}$ may not be important for the uptake of H_2O_2 and PAA.

Both PAA and H_2O_2 have strong oxidative capacity and can react with the reducing substances on aerosol particles, especially in the presence of water. Zhao et al. (2013) found that $\gamma_{H_2O_2}$ on sulfite-coated calcium carbonate particles is 3–10 times higher than that on the pristine calcium carbonate particles. This enhancement increased with increasing RH.
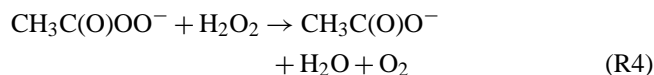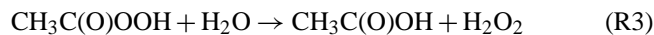
In addition, transition metals make up 0.9 % of $PM_{2.5}$ mass on haze days and 1.2 % on non-haze days. Both PAA and H_2O_2 can undergo catalytic reactions with transition metals, leading to the formation of highly reactive species, such as OH, RO and RO_2 radicals (Koubek and Edwards, 1963; Lin and Gurol, 1998; Zhang et al., 1998; Hiroki and LaVerne, 2005). Nawrot et al. (2009) have studied $PM_{2.5}$ samples in 20 European locations and suggested that H_2O_2 would decompose and form OH radicals in the presence of transition metals (e.g., Cu, Fe, Mn, V and Ti). Petigara et al. (2002) have reported that the decomposition rate of H_2O_2 is enhanced by the presence of organic matter and manganese. Therefore, the redox reactions may be important to the uptake of peroxide compounds on $PM_{2.5}$.

It is noted that PAA, which has a hydroperoxyl group (-OOH) and a carbonyl group (C = O), is less stable than H_2O_2 (Kunigk et al., 2012) and can more readily undergo thermal decomposition. The O–O bond dissociation enthalpies at 298 K of PAA and H_2O_2 are 48 and 50 kcal mol^{-1}, respectively (Bach et al., 1996). In addition, PAA is prone to hydrolysis in the presence of water (reactions 3 and 4) (Yuan et al., 1997). This is consistent with our experimental result that $R_{\gamma PAA}$ is larger than $R_{\gamma H_2O_2}$.

$$CH_3C(O)OOH + H_2O \rightarrow CH_3C(O)OH + H_2O_2 \qquad (R3)$$

$$CH_3C(O)OO^- + H_2O_2 \rightarrow CH_3C(O)O^- \\ + H_2O + O_2 \qquad (R4)$$

In considering the role of aqueous reactions, water-soluble inorganic salts including sulfate and nitrate make up a substantial fraction (35–58 %) of PM$_{2.5}$ (Sun et al., 2004; Wang et al., 2005). As shown in Table 5, the concentration of Cl$^-$, NO$_3^-$ and SO$_4^{2-}$ accounts for 61.9 and 42.0 % of PM$_{2.5}$ mass on haze days and non-haze days, respectively. These salts can greatly increase the water content of the particles under humid conditions. When RH exceeds the deliquescence relative humidity (DRH) of these inorganic salts, PM$_{2.5}$ may be covered with an aqueous film on the particle surface or exist in a liquid phase state. The DRH is suggested to be 79 % for (NH$_4$)$_2$SO$_4$, 39 % for NH$_4$HSO$_4$ and 62 % for NH$_4$NO$_3$ at 298 K (Cziczo et al., 1997; Lightstone et al., 2000), and the DRH of PM$_{2.5}$ is even lower than that of the individual salt particles (Seinfeld and Pandis, 2006). Under humid conditions, the deliquesced particles and/or the aqueous film on the particle surface becomes a medium for aqueous reaction. In this aqueous phase, soluble salts will release anions. The anions can potentially enhance the dissolution of Fe minerals (Rubasinghege et al., 2010), resulting in a larger uptake of peroxide compounds by Fe catalysis (Chevallier et al., 2004; Pignatello et al., 2006). Furthermore, Zhao et al. (2013) have provided experimental evidence for the effect of a soluble salt on $\gamma_{H_2O_2}$. They found that nitrate coated on calcium carbonate particles decreased the $\gamma_{H_2O_2}$ by 30–85 % at 3 % RH, but increases $\gamma_{H_2O_2}$ by a factor of 1–8 with increasing RH from 20 to 75 %, as compared to the $\gamma_{H_2O_2}$ on the uncoated particles. Mineral dust can undergo atmospheric aging from its emission, which modifies its surface with coating sulfates and nitrates (Sullivan et al., 2007). The aged authentic mineral dust particles (e.g., ADS dust, Gobi dust and Saharan dust) are coated with salts, while the mineral oxide (e.g., SiO$_2$, TiO$_2$ and α–Al$_2$O$_3$) and ATD particles have no or few soluble salt coatings. For example, in this study, the measured concentration of SO$_4^{2-}$ in ADS and ATD particles was 20.3 and 0.2 µg mg^{-1}, respectively. The coatings on the particles can lead to the formation of a surface aqueous film, in which the aqueous reactions may occur. This observation helps explain the differences in RH dependence of the uptake of peroxides on aged authentic particles and unaged mineral oxide and ATD particles. In short, the aqueous reactions that occur in the aqueous film or liquid particles formed by the deliquescence of soluble salts may play important roles in the uptake of peroxide compounds on PM$_{2.5}$ and aged mineral dust particles.

In summary, chemical processes rather than physical processes dominate the heterogeneous reaction of peroxide compounds on PM$_{2.5}$ and aged mineral dust particles. The soluble inorganic components in authentic particles play an important role in the uptake of peroxide compounds. The uptake of peroxide compounds on PM$_{2.5}$ is probably affected by the combined effects of catalytic reactions, redox reactions, thermal decomposition, and aqueous reactions.

4 Conclusions and implications

The present study is the first to measure the uptake coefficient of gaseous PAA and H_2O_2 on ambient PM$_{2.5}$ and on mineral dust over a wide range of RH values (3–90 %). Both γ_{PAA} and $\gamma_{H_2O_2}$ on PM$_{2.5}$ have a positive correlation with RH. In general, both γ_{PAA} and $\gamma_{H_2O_2}$ are on the order of 10^{-4}. The γ_{PAA} values show no obvious differences between haze days and non-haze days. Both γ_{PAA} and $\gamma_{H_2O_2}$ on Asian Dust storm (ADS) particles show a similar RH dependence compared to PM$_{2.5}$, but on Arizona Test Dust (ATD), both γ_{PAA} and $\gamma_{H_2O_2}$ show a negative RH dependence. This observation provides evidence that, in addition to the mineral dust, other components in PM$_{2.5}$, such as soluble inorganic salts and organic compounds, may greatly contribute to the uptake of peroxide compounds. The ratio of $\gamma_{PAA,90\%RH}$ to $\gamma_{PAA,3\%RH}$ ($R_{\gamma PAA}$) is larger than the ratio of $\gamma_{H_2O_2,90\%RH}$ to $\gamma_{H_2O_2,3\%RH}$ ($R_{\gamma H_2O_2}$), while the Henry's law constant of H_2O_2 is 100 times that of PAA; besides, authentic particles show a sustained surface reactivity for the uptake of peroxide compounds. These two experimental results suggest that chemical processes dominate the uptake of peroxide compounds onto PM$_{2.5}$ and aged mineral dust. The potential chemical processes include catalytic reactions, redox reactions, thermal decomposition and aqueous reactions. The heterogeneous processes of H_2O_2 have already been taken into account as an important removal pathway (de Reus et al., 2005; Liang et al., 2013). To the best of our knowledge, there has been almost no consideration of the heterogeneous removal pathways for organic peroxides.

Field observations have shown that the atmospheric lifetime of PAA is 4.1–5.8 h in summer in Beijing (Zhang et al., 2010; Liang et al., 2013). To explain this result, we at first considered the traditional removal mechanism for PAA, including the gas phase chemical reactions (OH radical reaction and photolysis) and deposition (Jackson and Hewitt, 1999). The concentration of OH radicals has a positive correlation with solar ultraviolet irradiation and changes in different seasons. The mean concentration of OH radicals on a non-haze summer day was estimated as 3.4×10^6 molecule cm^{-3} in the 35–45° N area (Bahm

and Khalil, 2004), where Beijing is located. In addition, the concentration of OH radicals on a haze day is one-fourth of that on a non-haze day (Liang et al., 2013). The reaction rate constant of OH radicals with PAA is $3.7 \times 10^{-12} \, \mathrm{cm^3 \, molecule^{-1} \, s^{-1}}$ (Jenkin et al., 1997; Saunders et al., 2003). Hence, the lifetime of PAA with respect to the OH radical reaction is 88.3 h on a haze day and 22.1 h on a non-haze day. Using the reported cross sections of PAA by Orlando and Tyndall (2003), the lifetime of PAA against photolysis is about 28 days on haze days and 21 days on non-haze days. In these studies, we assume that the planetary boundary layer is 1000 m and the dry deposition of PAA is $0.27 \, \mathrm{cm \, s^{-1}}$ (Wesely, 1989; Hall et al., 1999), both on haze and non-haze days. The lifetime of PAA against dry deposition is 4.3 days. The estimated overall lifetime of PAA is 44.2 h on a haze day and 17.6 h on a non-haze day. Obviously, this lifetime is much longer than the field observation results, especially on haze days, indicating that the heterogeneous reaction of PAA on ambient particles would be a removal pathway for gaseous PAA.

In order to estimate the PAA lifetime with respect to the heterogeneous reactions, we assume that all $PM_{2.5}$ particles are spheres and the heterogeneous reaction of PAA on $PM_{2.5}$ is a pseudo-first-order reaction. The lifetime of PAA can be calculated by Eq. (20) (Ravishankara, 1997):

$$\tau = \frac{[C]}{\mathrm{d}[C]/\mathrm{d}t} = \frac{4}{\gamma \omega A_v}, \tag{20}$$

where A_v is the surface area per unit volume of $PM_{2.5}$, $\mathrm{m^2 \, m^{-3}}$. Assuming each mode of aerosol fine particles is a log-normal distribution, the particles number can be expressed as Eq. (21) (Seinfeld and Pandis, 2006):

$$\frac{\mathrm{d}N}{\mathrm{d}\log D_p} = $$
$$\sum_i^n \frac{N_i}{\sqrt{2\pi} \log \sigma_i} \exp\left(\frac{(\log D_p - \log \overline{D_{p_i}})^2}{2\log^2 \sigma_i}\right), \tag{21}$$

where $i = 1, 2, 3$ correspond to the nucleation mode (3–20 nm), Aiken mode (20–100 nm), and accumulation mode (100–1000 nm), respectively; N_i is the number concentration; $\overline{D_{p_i}}$ is the geometric mean diameter, m; σ_i is the geometric standard deviation of the ith mode. The recommended values of $N_{t,i}$, $\overline{D_{p_i}}$ and σ_i are suggested by Yue et al. (2009). The value of A_v can be calculated by Eq. (22):

$$A_v = \frac{6M_a}{\rho \overline{D_p} V}, \tag{22}$$

where M_a is the mass of the $PM_{2.5}$ particles, kg; ρ is the density of the $PM_{2.5}$ particles, $1.42 \times 10^3 \, \mathrm{kg \, m^{-3}}$ for a haze period and $1.96 \times 10^3 \, \mathrm{kg \, m^{-3}}$ for a non-haze period (Hu et al., 2012); $\overline{D_p}$ is the mean diameter of the total particles, m; and V is the volume of sampling air, $\mathrm{m^3}$. The number

percentage of coarse mode particles (1000–2500 nm) is less than 0.02 % of the fine particle number (3–1000 nm) (Wu et al., 2008) and the corresponding surface area of the coarse mode is about 0.4 % of the total surface area. Therefore, the surface area of the coarse mode particles (1000–2500 nm) could be negligible and $\overline{D_p}$ is 114.6 nm for haze-day $PM_{2.5}$ particles and 62.4 nm for non-haze $PM_{2.5}$ particles. The mean mass concentration is $123 \, \mathrm{\mu g \, m^{-3}}$ on a haze day and $23 \, \mathrm{\mu g \, m^{-3}}$ on a non-haze day and the corresponding A_v is $4.5 \times 10^3 \, \mathrm{\mu m^2 \, cm^{-3}}$ on a haze day and $1.2 \times 10^3 \, \mathrm{\mu m^2 \, cm^{-3}}$ on a non-haze day, which is similar to the literature results (Wehner et al., 2008; He et al., 2010). Here, we use the mean uptake coefficient of PAA on $PM_{2.5}$ at 60 % RH, i.e., $\gamma = 2.70 \times 10^{-4}$, to estimate the lifetime of PAA. The calculated lifetime of PAA against heterogeneous reaction is 3.2 h on a haze day and 11.9 h on a non-haze day, which are more important than photolysis and decomposition and can compete with OH reaction on haze days. Considering heterogeneous reaction, gas phase reaction and deposition, the estimated lifetime of PAA is 3.0 h on a haze day and 7.1 h on a non-haze day, which is similar to the field measurement results. Thus, the heterogeneous reaction on $PM_{2.5}$ is likely to be an important removal pathway for PAA.

The fate of peroxide compounds on aerosols will greatly impact the budget of peroxide compounds themselves as well as the cycle of radicals in the atmosphere. The formation of PAA and H_2O_2 is related to the self-reaction of HO_2 radical and the reaction of HO_2 radicals with RO_2 radicals, while the photolysis of PAA and H_2O_2 releases HO_x radicals and RO_x radicals. Therefore, peroxide compounds can be treated as a temporary reservoir of HO_x radicals and RO_x radicals. Besides, PAA has a close relation with peroxyacetyl nitrate (PAN). In high NO_x ($NO + NO_2$) areas, such as urban areas, NO_2 will combine with acetyl peroxy ($CH_3C(O)OO$) radicals to form PAN by competing with HO_2 radicals that will donate H to the $CH_3C(O)OO$ radical to form PAA. The uptake of PAA onto the particle surface will result in a sink for the $CH_3C(O)OO$ radical, hence reducing PAN, which is an important carrier of NO_x and regionally transports NO_x from urban areas to rural and remote areas, affecting oxidant (e.g., O_3 and OH radical) distribution there (Fischer et al., 2014). Moreover, through the heterogeneous uptake, the peroxide compounds are introduced onto the surface of particles, which might enhance the atmospheric aerosol oxidative capacity and then change the composition of the aerosols. For example, Zhao et al. (2014) have suggested that the co-existence of H_2O_2 could enhance heterogeneous oxidation of OVOCs and the yield of organic acids, such as formic acid and acetic acid. Moreover, peroxide compounds have the potential to enhance the heterogeneous reaction of SO_2 and promote sulfate formation. Hence, the heterogeneous reaction of peroxide compounds on aerosols may help to explain the high concentration of sulfates during haze episodes when other oxidants (e.g., OH radicals) are limited. Therefore, we suggest that the current atmospheric models should take into

account the heterogeneous reactions of peroxide compounds on aerosols.

References

Atkinson, R., Aschmann, S. M., Arey, J., and Shorees, B.: Formation of OH radicals in the gas phase reactions of O$_3$ with a series of terpenes, J. Geophys. Res., 97, 6065–6073, doi:10.1029/92jd00062, 1992.

Bach, R. D., Ayala, P. Y., and Schlegel, H. B.: A reassessment of the bond dissociation energies of peroxides. An ab Initio Study, J. Am. Chem. Soc., 118, 12758–12765, doi:10.1021/ja961838i, 1996.

Bahm, K. and Khalil, M. A. K.: A new model of tropospheric hydroxyl radical concentrations, Chemosphere, 54, 143–166, doi:10.1016/j.chemosphere.2003.08.006, 2004.

Bedjanian, Y., Romanias, M. N., and El Zein, A.: Uptake of HO$_2$ radicals on Arizona Test Dust, Atmos. Chem. Phys., 13, 6461–6471, doi:10.5194/acp-13-6461-2013, 2013.

Calvert, J. G., Lazrus, A., Kok, G. L., Heikes, B. G., Walega, J. G., Lind, J., and Cantrell, C. A.: Chemical mechanisms of acid generation in the troposphere, Nature, 317, 27–35, doi:10.1038/317027a0, 1985.

Chevallier, E., Jolibois, R. D., Meunier, N., Carlier, P., and Monod, A.: "Fenton-like" reactions of methylhydroperoxide and ethylhydroperoxide with Fe^{2+} in liquid aerosols under tropospheric conditions, Atmos. Environ., 38, 921–933, doi:10.1016/j.atmosenv.2003.10.027, 2004.

Claeys, M., Wang, W., Ion, A. C., Kourtchev, I., Gelencsér, A., and Maenhaut, W.: Formation of secondary organic aerosols from isoprene and its gas-phase oxidation products through reaction with hydrogen peroxide, Atmos. Environ., 38, 4093–4098, doi:10.1016/j.atmosenv.2004.06.001, 2004.

Crowley, J. N., Ammann, M., Cox, R. A., Hynes, R. G., Jenkin, M. E., Mellouki, A., Rossi, M. J., Troe, J., and Wallington, T. J.: Evaluated kinetic and photochemical data for atmospheric chemistry: Volume V – heterogeneous reactions on solid substrates, Atmos. Chem. Phys., 10, 9059–9223, doi:10.5194/acp-10-9059-2010, 2010.

Cziczo, D. J., Nowak, J. B., Hu, J. H., and Abbatt, J. P. D.: Infrared spectroscopy of model tropospheric aerosols as a function of relative humidity: Observation of deliquescence and crystallization, J. Geophys. Res., 102, 18843–18850, doi:10.1029/97jd01361, 1997.

de Reus, M., Fischer, H., Sander, R., Gros, V., Kormann, R., Salisbury, G., Van Dingenen, R., Williams, J., Zöllner, M., and Lelieveld, J.: Observations and model calculations of trace gas scavenging in a dense Saharan dust plume during MINATROC,

Atmos. Chem. Phys., 5, 1787–1803, doi:10.5194/acp-5-1787-2005, 2005.

Docherty, K. S., Wu, W., Lim, Y. B., and Ziemann, P. J.: Contributions of organic peroxides to secondary aerosol formed from reactions of monoterpenes with O$_3$, Environ. Sci. Technol., 39, 4049–4059, doi:10.1021/es050228s, 2005.

Dul'neva, L. V. and Moskvin, A. V.: Kinetics of formation of peroxyacetic acid, Russ. J. Gen. Chem., 75, 1125–1130, doi:10.1007/s11176-005-0378-8, 2005.

Eldred, R. A., Cahill, T. A., and Flocchini, R. G.: Composition of PM$_{2.5}$ and PM$_{10}$ aerosols in the IMPROVE Network, J. Air Waste Manage., 47, 194–203, doi:10.1080/10473289.1997.10464422, 1997.

El Zein, A., Romanias, M. N., and Bedjanian, Y.: Heterogeneous interaction of H$_2$O$_2$ with Arizona Test Dust, J. Phys. Chem. A, 118, 441–448, doi:10.1021/jp409946j, 2014.

Evans, D. F. and Upton, M. W.: Studies on singlet oxygen in aqueous solution. Part 3. The decomposition of peroxy-acids, J. Chem. Soc. Dalton, 1985, 1151–1153, doi:10.1039/dt9850001151, 1985.

Fischer, E. V., Jacob, D. J., Yantosca, R. M., Sulprizio, M. P., Millet, D. B., Mao, J., Paulot, F., Singh, H. B., Roiger, A., Ries, L., Talbot, R.W., Dzepina, K., and Pandey Deolal, S.: Atmospheric peroxyacetyl nitrate (PAN): a global budget and source attribution, Atmos. Chem. Phys., 14, 2679–2698, doi:10.5194/acp-14-2679-2014, 2014.

Hall, B., Claiborn, C., and Baldocchi, D.: Measurement and modeling of the dry deposition of peroxides, Atmos. Environ., 33, 577–589, doi:10.1016/s1352-2310(98)00271-4, 1999.

He, K., Yang, F., Ma, Y., Zhang, Q., Yao, X., Chan, C. K., Cadle, S., Chan, T., and Mulawa, P.: The characteristics of PM$_{2.5}$ in Beijing, China, Atmos. Environ., 35, 4959–4970, doi:10.1016/s1352-2310(01)00301-6, 2001.

He, S. Z., Chen, Z. M., Zhang, X., Zhao, Y., Huang, D. M., Zhao, J. N., Zhu, T., Hu, M., and Zeng, L. M.: Measurement of atmospheric hydrogen peroxide and organic peroxides in Beijing before and during the 2008 Olympic Games: Chemical and physical factors influencing their concentrations, J. Geophys. Res., 115, D17307, doi:10.1029/2009jd013544, 2010.

Hiroki, A. and LaVerne, J. A.: Decomposition of hydrogen peroxide at water-ceramic oxide interfaces, J. Phys. Chem. B, 109, 3364–3370, doi:10.1021/jp046405d, 2005.

Hu, M., Peng, J., Sun, K., Yue, D., Guo, S., Wiedensohler, A., and Wu, Z.: Estimation of size-Resolved ambient particle density based on the measurement of aerosol number, mass, and chemical size distributions in the winter in Beijing, Environ. Sci. Technol., 46, 9941–9947, doi:10.1021/es204073t, 2012.

Hua, W., Chen, Z. M., Jie, C. Y., Kondo, Y., Hofzumahaus, A., Takegawa, N., Chang, C. C., Lu, K. D., Miyazaki, Y., Kita, K., Wang, H. L., Zhang, Y. H., and Hu, M.: Atmospheric hydrogen peroxide and organic hydroperoxides during PRIDE-PRD'06, China: their concentration, formation mechanism and contribution to secondary aerosols, Atmos. Chem. Phys., 8, 6755–6773, doi:10.5194/acp-8-6755-2008, 2008.

Huang, D., Chen, Z. M., Zhao, Y., and Liang, H.: Newly observed peroxides and the water effect on the formation and removal of hydroxyalkyl hydroperoxides in the ozonolysis of isoprene, Atmos. Chem. Phys., 13, 5671–5683, doi:10.5194/acp-13-5671-2013, 2013.

Huang, X. H. H., Bian, Q. J., Ng, W. M., Louie, P. K. K., and Yu, J. Z.: Characterization of $PM_{2.5}$ major components and source investigation in suburban Hong Kong: A one year monitoring study, Aerosol Air Qual. Res., 14, 237–250, doi:10.4209/aaqr.2013.01.0020, 2014.

Hueglin, C., Gehrig, R., Baltensperger, U., Gysel, M., Monn, C., and Vonmont, H.: Chemical characterisation of $PM_{2.5}$, PM_{10} and coarse particles at urban, near-city and rural sites in Switzerland, Atmos. Environ., 39, 637–651, doi:10.1016/j.atmosenv.2004.10.027, 2005.

Jackson, A. V. and Hewitt, C. N.: Atmosphere hydrogen peroxide and organic hydroperoxides: a review, Crit. Rev. Env. Sci. Tec., 29, 175–228, doi:10.1080/10643389991259209, 1999.

Jenkin, M. E., Saunders, S. M., and Pilling, M. J.: The tropospheric degradation of volatile organic compounds: a protocol for mechanism development, Atmos. Environ., 31, 81–104, doi:10.1016/s1352-2310(96)00105-7, 1997.

Koubek, E. and Edwards, J. O.: The formation of cobaltic acetate in the catalytic decomposition of peroxyacetic acid, J. Inorg. Nucl. Chem., 25, 1401–1408, doi:10.1016/0022-1902(63)80411-x, 1963.

Kunigk, L., Silva, S. M., and Jurkiewicz, C. H.: The Influence of temperature and organic matter on the decomposition kinetics of peracetic acid in aqueous solutions, Lat. Am. Appl. Res., 42, 291–297, doi:10.1590/S0104-66322001000200009, 2012.

Lee, M., Noone, B. C., O'sullivan, D., and Heikes, B. G.: Method for the collection and HPLC analysis of hydrogen-peroxide and C_1 and C_2 hydroperoxides in the atmosphere, J. Atmos. Ocean. Tech., 12, 1060–1070, doi:10.1175/1520-0426(1995)012<1060:mftcah>2.0.co;2, 1995.

Lee, M. H., Heikes, B. G., and O'Sullivan, D. W.: Hydrogen peroxide and organic hydroperoxide in the troposphere: a review, Atmos. Environ., 34, 3475–3494, doi:10.1016/s1352-2310(99)00432-x, 2000.

Li, W.: Fundamentals of Aerosol Pollution Chemistry, Yellow River Conservancy Press, Zheng Zhou, 2010.

Liang, H., Chen, Z. M., Huang, D., Zhao, Y., and Li, Z. Y.: Impacts of aerosols on the chemistry of atmospheric trace gases: a case study of peroxides and HO_2 radicals, Atmos. Chem. Phys., 13, 11259–11276, doi:10.5194/acp-13-11259-2013, 2013.

Lightfoot, P. D., Roussel, P., Caralp, F., and Lesclaux, R.: Flash-photolysis study of the $CH_3O_2 + CH_3O_2$ and $CH_3O_2 + HO_2$ reactions between 600 and 719 K: unimolecular decompositionof methylhydroperoxide, J. Chem. Soc. Farad., 87, 3213–3220, doi:10.1039/FT9918703213, 1991.

Lightstone, J. M., Onasch, T. B., Imre, D., and Oatis, S.: Deliquescence, efflorescence, and water activity in ammonium nitrate and mixed ammonium nitrate/succinic acid microparticles, J. Phys. Chem. A, 104, 9337–9346, doi:10.1021/jp002137h, 2000.

Lin, S. S. and Gurol, M. D.: Catalytic decomposition of hydrogen peroxide on iron oxide: Kinetics, mechanism, and implications, Environ. Sci. Technol., 32, 1417–1423, doi:10.1021/es970648k, 1998.

Lind, J. A., Lazrus, A. L., and Kok, G. L.: Aqueous phase oxidation of sulfur(IV) by hydrogen peroxide, methylhydroperoxide, and peroxyacetic acid, J. Geophys. Res., 92, 4171–4177, doi:10.1029/JD092iD04p04171, 1987.

Marinoni, A., Parazols, M., Brigante, M., Deguillaume, L., Amato, P., Delort, A. M., Laj, P., and Mailhot, G.: Hydrogen peroxide in natural cloud water: sources and photoreactivity, Atmos. Res., 101, 256–263, doi:10.1016/j.atmosres.2011.02.013, 2011.

Molina, M. J., Molina, L. T., and Golden, D. M.: Environmental Chemistry (Gas and Gas-Solid Interactions): The Role of Physical Chemistry, J. Phys. Chem., 100, 12888–12896, doi:10.1021/jp960146d, 1996.

Nawrot, T. S., Kuenzli, N., Sunyer, J., Shi, T., Moreno, T., Viana, M., Heinrich, J., Forsberg, B., Kelly, F. J., Sughis, M., Nemery, B., and Borm, P.: Oxidative properties of ambient $PM_{2.5}$ and elemental composition: Heterogeneous associations in 19 European cities, Atmos. Environ., 43, 4595–4602, doi:10.1016/j.atmosenv.2009.06.010, 2009.

Orlando, J. J. and Tyndall, G. S.: Gas phase UV absorption spectra for peracetic acid, and for acetic acid monomers and dimers, J. Photochem. Photobio. A, 157, 161–166, doi:10.1016/s1010-6030(03)00067-4, 2003.

O'Sullivan, D. W., Lee, M., Noone, B. C., and Heikes, B. G.: Henry's law constant determinations for hydrogen peroxide, methyl hydroperoxide, hydroxymethyl hydroperoxide, ethyl hydroperoxide, and peroxyacetic acid, J. Phys. Chem., 100, 3241–3247, doi:10.1021/jp951168n, 1996.

Paulot, F., Crounse, J. D., Kjaergaard, H. G., Kurten, A., St Clair, J. M., Seinfeld, J. H., and Wennberg, P. O.: Unexpected epoxide formation in the gas-phase photooxidation of isoprene, Science, 325, 730–733, doi:10.1126/science.1172910, 2009.

Petigara, B. R., Blough, N. V., and Mignerey, A. C.: Mechanisms of hydrogen peroxide decomposition in soils, Environ. Sci. Technol., 36, 639–645, doi:10.1021/es001726y, 2002.

Phillips, G. J., Pouvesle, N., Thieser, J., Schuster, G., Axinte, R., Fischer, H., Williams, J., Lelieveld, J., and Crowley, J. N.: Peroxyacetyl nitrate (PAN) and peroxyacetic acid (PAA) measurements by iodide chemical ionisation mass spectrometry: first analysis of results in the boreal forest and implications for the measurement of PAN fluxes, Atmos. Chem. Phys., 13, 1129–1139, doi:10.5194/acp-13-1129-2013, 2013.

Pignatello, J. J., Oliveros, E., and MacKay, A.: Advanced oxidation processes for organic contaminant destruction based on the Fenton reaction and related chemistry, Crit. Rev. Env. Sci. Tec., 36, 1–84, doi:10.1080/10643380500326564, 2006.

Pradhan, M., Kalberer, M., Griffiths, P. T., Braban, C. F., Pope, F. D., Cox, R. A., and Lambert, R. M.: Uptake of gaseous hydrogen peroxide by submicrometer titanium dioxide aerosol as a function of relative humidity, Environ. Sci. Technol., 44, 1360–1365, doi:10.1021/Es902916f, 2010a.

Pradhan, M., Kyriakou, G., Archibald, A. T., Papageorgiou, A. C., Kalberer, M., and Lambert, R. M.: Heterogeneous uptake of gaseous hydrogen peroxide by Gobi and Saharan dust aerosols: a potential missing sink for H_2O_2 in the troposphere, Atmos. Chem. Phys., 10, 7127–7136, doi:10.5194/acp-10-7127-2010, 2010b.

Preszler P. A., Grassian, V. H., Kleiber, P., and Young, M. A.: Heterogeneous conversion of calcite aerosol by nitric acid, Phys. Chem. Chem. Phys., 9, 622–634, doi:10.1039/b613913b, 2007.

Ravetta, F., Jacob, D. J., Brune, W. H., Heikes, B. G., Anderson, B. E., Blake, D. R., Gregory, G. L., Sachse, G. W., Sandholm, S. T., Shetter, R. E., Singh, H. B., and Talbot, R. W.: Experimental evidence for the importance of convected methylhydroperoxide as a source of hydrogen oxide (HO_x) radicals in the trop-

ical upper troposphere, J. Geophys. Res., 106, 32709–32716, doi:10.1029/2001jd900009, 2001.

Ravishankara, A. R.: Heterogeneous and multiphase chemistry in the troposphere, Science, 276, 1058–1065, doi:10.1126/science.276.5315.1058, 1997.

Reeves, C. E. and Penkett, S. A.: Measurements of peroxides and what they tell us, Chem. Rev., 103, 5199–5218, doi:10.1021/cr0205053, 2003.

Romanias, M. N., El Zein, A., and Bedjanian, Y.: Heterogeneous interaction of H_2O_2 with TiO_2 surface under dark and UV light irradiation conditions, J. Phys. Chem. A, 116, 8191–8200, doi:10.1021/jp305366v, 2012.

Romanias, M. N., El Zein, A., and Bedjanian, Y.: Uptake of hydrogen peroxide on the surface of Al_2O_3 and Fe_2O_3, Atmos. Environ., 77, 1–8, doi:10.1016/j.atmosenv.2013.04.065, 2013.

Rubasinghege, G., Lentz, R. W., Scherer, M. M., and Grassian, V. H.: Simulated atmospheric processing of iron oxyhydroxide minerals at low pH: roles of particle size and acid anion in iron dissolution, P. Natl. Acad. Sci. USA, 107, 6628–6633, doi:10.1073/pnas.0910809107, 2010.

Santschi, C. and Rossi, M. J.: Uptake of CO_2, SO_2, HNO_3 and HCl on calcite ($CaCO_3$) at 300 K: mechanism and the role of adsorbed water, J. Phys. Chem. A, 110, 6789–6802, doi:10.1021/jp056312b, 2006.

Saunders, S. M., Jenkin, M. E., Derwent, R. G., and Pilling, M. J.: Protocol for the development of the Master Chemical Mechanism, MCM v3 (Part A): tropospheric degradation of non-aromatic volatile organic compounds, Atmos. Chem. Phys., 3, 161–180, doi:10.5194/acp-3-161-2003, 2003.

Seinfeld, J. H. and Pandis, S. N.: Atmospheric chemistry and physics: From air pollution to climate change, John Wiley & Sons, 2006.

Shen, X. L., Zhao, Y., Chen, Z. M., and Huang, D.: Heterogeneous reactions of volatile organic compounds in the atmosphere, Atmos. Environ., 68, 297–314, doi:10.1016/j.atmosenv.2012.11.027, 2013.

Stein, A. F. and Saylor, R. D.: Sensitivities of sulfate aerosol formation and oxidation pathways on the chemical mechanism employed in simulations, Atmos. Chem. Phys., 12, 8567–8574, doi:10.5194/acp-12-8567-2012, 2012.

Sullivan, R. C., Guazzotti, S. A., Sodeman, D. A., and Prather, K. A.: Direct observations of the atmospheric processing of Asian mineral dust, Atmos. Chem. Phys., 7, 1213–1236, doi:10.5194/acp-7-1213-2007, 2007.

Sullivan, R. C., Moore, M. J. K., Petters, M. D., Kreidenweis, S. M., Roberts, G. C., and Prather, K. A.: Timescale for hygroscopic conversion of calcite mineral particles through heterogeneous reaction with nitric acid, Phys. Chem. Chem. Phys., 11, 7826–7837, doi:10.1039/b904217b, 2009.

Sun, Y., Zhuang, G., Wang, Y., Han, L., Guo, J., Dan, M., Zhang, W., Wang, Z., and Hao, Z.: The air-borne particulate pollution in Beijing – concentration, composition, distribution and sources, Atmos. Environ., 38, 5991–6004, doi:10.1016/j.atmosenv.2004.07.009, 2004.

Sun, Y., Zhuang, G., Tang, A., Wang, Y., and An, Z.: Chemical characteristics of $PM_{2.5}$ and PM_{10} in haze-fog episodes in Beijing, Environ. Sci. Technol., 40, 3148–3155, doi:10.1021/es051533g, 2006.

Surratt, J. D., Murphy, S. M., Kroll, J. H., Ng, N. L., Hildegrandt, L., Sorooshian, A., Szmigielski, R., Vermeylen, R., Maenhaut, W., Claeys, M., Flagan, R., and Seinfeld, J. H.: Chemical compositionof secondary organic aerosol formed from the photooxidationof isoprene, J. Phys. Chem. A., 110, 9665–9690, doi:10.1021/jp061734m, 2006.

Vaghjiani, G. L. and Ravishankara, A. R.: Photodissociation of H_2O_2 and CH_3OOH at 248 nm and 298 K: Quantum yields for OH, $O(^3P)$ and $H(^2S)$, J. Chem. Phys., 92, 996–1003, doi:10.1063/1.458081, 1990.

Wang, W. G., Ge, M. F., and Sun, Q.: Heterogeneous uptake of hydrogen peroxide on mineral oxides, Chinese J. Chem. Phys., 24, 515–520, doi:10.1088/1674-0068/24/05/515-520, 2011.

Wang, Y., Zhuang, G., Tang, A., Yuan, H., Sun, Y., Chen, S., and Zheng, A.: The ion chemistry and the source of $PM_{2.5}$ aerosol in Beijing, Atmos. Environ., 39, 3771–3784, doi:10.1016/j.atmosenv.2005.03.013, 2005.

Wallington, T. J. and Japar, S. M.: Reaction of $CH_3O_2 + HO_2$ in air at 295 K: a product study, Chem. Phys. Lett., 167, 513–518, doi:10.1016/0009-2614(90)85461-K, 1990.

Wehner, B., Birmili, W., Ditas, F., Wu, Z., Hu, M., Liu, X., Mao, J., Sugimoto, N., and Wiedensohler, A.: Relationships between submicrometer particulate air pollution and air mass history in Beijing, China, 2004–2006, Atmos. Chem. Phys., 8, 6155–6168, doi:10.5194/acp-8-6155-2008, 2008.

Wesely, M.: Parameterization of surface resistances to gaseous dry deposition in regional-scale numerical models, Atmos. Environ., 23, 1293–1304, doi:10.1016/0004-6981(89)90153-4, 1989.

Wu, Z., Hu, M., Lin, P., Liu, S., Wehner, B., and Wiedensohler, A.: Particle number size distribution in the urban atmosphere of Beijing, China, Atmos. Environ., 42, 7967–7980, doi:10.1016/j.atmosenv.2008.06.022, 2008.

Xu, L., Kollman, M. S., Song, C., Shilling, J. E., and Ng, N. L.: Effects of NO_x on the volatility of secondary organic aerosol from isoprene photooxidation, Environ. Sci. Technol., 48, 2253–2262, doi:10.1021/es404842g, 2014.

Yang, F., Tan, J., Zhao, Q., Du, Z., He, K., Ma, Y., Duan, F., Chen, G., and Zhao, Q.: Characteristics of $PM_{2.5}$ speciation in representative megacities and across China, Atmos. Chem. Phys., 11, 5207–5219, doi:10.5194/acp-11-5207-2011, 2011.

Yuan, Z., Ni, Y., and Van Heiningen, A. R. P.: Kinetics of the peracetic acid decomposition: Part II: pH effect and alkaline hydrolysis, Can. J. Chem. Eng., 75, 42–47, doi:10.1002/cjce.5450750109, 1997.

Yue, D., Hu, M., Wu, Z., Wang, Z., Guo, S., Wehner, B., Nowak, A., Achtert, P., Wiedensohler, A., Jung, J., Kim, Y. J., and Liu, S.: Characteristics of aerosol size distributions and new particle formation in the summer in Beijing, J. Geophys. Res., 114, D00G12, doi:10.1029/2008jd010894, 2009.

Zhang, R., Jing, J., Tao, J., Hsu, S.-C., Wang, G., Cao, J., Lee, C. S. L., Zhu, L., Chen, Z., Zhao, Y., and Shen, Z.: Chemical characterization and source apportionment of $PM_{2.5}$ in Beijing: seasonal perspective, Atmos. Chem. Phys., 13, 7053–7074, doi:10.5194/acp-13-7053-2013, 2013.

Zhang, X., Chen, Z. M., He, S. Z., Hua, W., Zhao, Y., and Li, J. L.: Peroxyacetic acid in urban and rural atmosphere: concentration, feedback on PAN-NO_x cycle and implication on radical chemistry, Atmos. Chem. Phys., 10, 737–748, doi:10.5194/acp-10-737-2010, 2010.

Zhang, X. Z., Francis, R. C., Dutton, D. B., and Hill, R. T.: Decomposition of peracetic acid catalyzed by cobalt(II) and vanadium(V), Can. J. Chem., 76, 1064–1069, doi:10.1139/v98-103, 1998.

Zhao, X. B., Zhang, T., Zhou, Y. J., and Liu, D. H.: Preparation of peracetic acid from hydrogen peroxide Part 1: Kinetics for peracetic acid synthesis and hydrolysis, J. Mol. Catal. A-Chem., 271, 246–252, doi:10.1016/j.molcata.2007.03.012, 2007.

Zhao, Y., Chen, Z., and Zhao, J.: Heterogeneous reactions of methacrolein and methyl vinyl ketone on α-Al$_2$O$_3$ particles, Environ. Sci. Technol., 44, 2035–2041, doi:10.1021/es9037275, 2010.

Zhao, Y., Chen, Z., Shen, X., and Zhang, X.: Kinetics and mechanisms of heterogeneous reaction of gaseous hydrogen peroxide on mineral oxide particles, Environ. Sci. Technol., 45, 3317–3324, doi:10.1021/es104107c, 2011a.

Zhao, Y., Chen, Z. M., Shen, X. L., and Huang, D.: Importance of atmospheric aging in reactivity of mineral dust aerosol: a case study of heterogeneous reaction of gaseous hydrogen peroxide on processed mineral particles, Atmos. Chem. Phys. Discuss., 11, 28563–28586, doi:10.5194/acpd-11-28563-2011, 2011b.

Zhao, Y., Chen, Z., Shen, X., and Huang, D.: Heterogeneous reactions of gaseous hydrogen peroxide on pristine and acidic gas-processed calcium carbonate particles: Effects of relative humidity and surface coverage of coating, Atmos. Environ., 67, 63–72, doi:10.1016/j.atmosenv.2012.10.055, 2013.

Zhao, Y., Huang, D., Huang, L., and Chen, Z.: Hydrogen peroxide enhances the oxidation of oxygenated volatile organic compounds on mineral dust particles: a case study of methacrolein, Environ. Sci. Technol., 48, 10614–10623, doi:10.1021/es5023416, 2014.

Zhao, Y., Wingen, L. M., Perraud, V., Greaves, J., and Finlayson-Pitts, B. J.: Role of the reaction of stabilized Criegee intermediates with peroxy radicals in particle formation and growth in air, Phys. Chem. Chem. Phys., 17, 12500–12514, doi:10.1039/c5cp01171j, 2015.

Zhou, L., Wang, W. G., and Ge, M. F.: Temperature dependence of heterogeneous uptake of hydrogen peroxide on silicon dioxide and calcium carbonate, J. Phys. Chem. A, 116, 7959–7964, doi:10.1021/jp304446y, 2012.